STRUCTURE OF SHOCK WAVES AND FUNDAMENTAL EQUATIONS FOR METALS

L. V. Al'tshuler and B. S. Chekin

UDC 534.222.2

1. Research Problem. The resistance of shock-compressed metals to shape change below the fusion line is described in [1-3] by alternative models for a relaxation [4, 5] or elastoplastic [3] medium. As mathematical modeling shows [1-7], for high velocity impact of a plate and reaction of shock waves (SW) with unloading waves, the results of experiments [3, 8-10] are adequately described in representations of Maxwellian relaxation and to the same extent by equations for a strengthening elastoplastic body taking account [3] of the Bauschinger effect blurring the unloading wave front.

The aim of the present work is determination on the basis of unambiguous experimental information of steady-state SW propagation for different shock-wave deformation conditions for aluminum and beryllium. The steady-state SW configurations reflect the main rheological parameters of the propagation medium, i.e., its effective viscosity, shear stress relaxation time, and dislocation characteristics. Recording of these values with different SW amplitudes is one of the main sources of information necessary for, constructing adequate fundamental equations (FE). With the accuracy required for this purpose, structures of the front have been recorded in aluminum [11] in the pressure range of 9 GPa, and in beryllium up to 25 GPa [12]. Limited information with upper estimates of front width have been obtained in [13] for some metals up to 100 GPa. Master data for deformation rates in the SW front have been obtained in a series of metals in [14].

2. Fundamental Equations and Dislocation Models. Metals and other crystalline bodies belong to materials with a "decaying memory." The magnitude of tangential stresses for them is a function of yield strength and relative rate of competing processes of shear deformation and plastic relaxation.

For planar flows the FE in the majority of studies overseas are written in the form of Malvern–Duval [15]

$$\dot{S} = \frac{4}{3}\mu\dot{e} - \frac{8}{3}\mu\dot{\gamma}^{p}, \tag{2.1}$$

convenient for representing the relaxation function by dislocation relationships. The most common phenomenological FE is the equation for a generalized Maxwellian liquid [4]

$$\dot{S} = \frac{4}{3}\mu\dot{e} - \frac{S}{t_p(S)}. \tag{2.2}$$

In (2.1) and (2.2) derivatives with respect to time for deviators $S = (4/3)\tau$ (τ is tangential stress), total unidimensional strain $e = \ln(\rho/\rho_0)$ (ρ_0 and ρ are initial and current density), and plastic shear deformation γ^p are labeled with periods. In both equations there is shear modulus μ, and in (2.2) there is relaxation function $t_p(S) = (\partial \ln S/\partial t)_e$ characterizing relaxation rate for viscous stresses with fixed strains.

For substances with pronounced critical shear stress τ^* with $S \geq S^* = 4\tau^*/3$

$$\dot{S} = \frac{4}{3}\mu\dot{e} - \frac{S - S^*}{t_p(S)} \tag{2.3}$$

On the basis of (2.1) and (2.3) effective viscosity of the medium

$$\eta = 2\mu t_p \tag{2.4}$$

Equation (2.3) contains plastic S^*, elastic μ, and relaxation t_p characteristics for the medium, and with variables $t_p(S)$ and $S^*(\gamma^p)$ it represents the most common model of deformation. In a special case with constants t_p and S^*, Eq. (2.3) relates to an ideal relaxing elastoplastic body, and with $S^* = 0$ it relates to an ideal Maxwellian liquid.

Moscow. Translated from Zhurnal Prikladnoi Mekhaniki i Tekhnicheskoi Fiziki, No. 6, pp. 119-128, November-December, 1987. Original article submitted July 30, 1986.

0021-8944/87/2806-0910$12.50

For quasisteady shape change regimes, if $\partial \ln \dot{e}/\partial t \ll t_p^{-1}$, neglecting $\dot{S}$, which is permissible under these conditions, converts (2.3) into a FE for a plastically viscous body

$$S = S^* + \frac{4}{3}\mu t_p \dot{e} = S + \frac{2}{3}\eta \dot{e} \tag{2.5}$$

with variable viscosity coefficient $\eta(\rho)$.

For "slow" processes with $\mu t_p \dot{e} \ll S^*$, (2.3) and (2.5) "degenerate" into a FE for a strengthening elastoplastic medium

$$S = S^* = (4/3)\tau^*, \tau = \tau(\gamma^p, T, p) \tag{2.6}$$

with critical tangential stress τ^* which is a function of plastic deformation γ^p, temperature T, and pressure p.

In crystalline bodies the predominant mechanism for deformation is a dislocation mechanism with a rate of plastic relaxation

$$\dot{\gamma}^p = bN_m v, \tag{2.7}$$

proportional to the density N_m of mobile dislocations, their average velocity v, and Burgers vector b; $\dot{\gamma}^p$ enters explicitly into the Malvern–Duval FE (2.1). In schematic description [16] relationship $v(\tau)$ for dislocation velocity includes critical stress at the start of flow τ^*, tangential stress range required for moving dislocations in a field of fine scale barriers, and the section of viscous movement over barriers with an upper relativistic limit equal to transverse sound velocity v_s. For many materials the significant initial region of the $v(\tau)$ curve with $\tau > \tau^*$ is satisfactorily described by a linear equation

$$v = b\tau_v/B, \tau_v = \tau - \tau^*,$$

where B is viscous retardation coefficient; τ_v is tangential stress viscous component. Relaxation rate (2.7) in the linear range

$$\dot{\gamma}^p = (N_m b^2/B)\tau_v. \tag{2.8}$$

whence

$$\eta_0 = B/(b^2 N_m), t_{p0} = B/(2\mu b^2 N_m). \tag{2.9}$$

For more complex relationships $v(\tau)$ taking account of the relativistic limitation of dislocation velocity by transverse sound velocity v_s, it is convenient to introduce according to [17] dimensionless velocity $\tilde{v} = v/v_s$ and stress $z = \tau/\tau_0$ relating to a unit of dislocation scale for tangential stresses

$$\tau_0 = v_s B/2b. \tag{2.10}$$

In these variables according to [17]

$$\tilde{v} = [(1 + z^2)^{1/2} - 1]/z. \tag{2.11}$$

Correspondingly

$$\eta/\eta_0 = t_p/t_{p0} = (1/2)z^2[(1 + z^2)^{1/2} - 1]. \tag{2.12}$$

For another class of materials with τ close to τ^*, dislocation velocity is controlled by the resistance of small-scale barriers which affect their movement. Depression of velocities with small z is described here by an equation close in structure to that in [11]

$$\tilde{v} = z^2(1 + z^2)^{-1} \tag{2.13}$$

and by relationships

$$\eta/\eta_0 = t_p/t_{p0} = (1/2)(z^2 + 1)/z. \tag{2.14}$$

For materials with these properties there is no separating boundary in shear stress values dividing elastic from viscoplastic behavior.

The main factor controlling the intensity of relaxation processes is in (2.7) the number of mobile dislocations $N_m = fN$ comprising the proportion f of their total density N; N_m is determined by competing processes of dislocation multiplication and their mutual blocking. In the simplest assumptions [11, 18] f = const and $N_m = N_{0m} = M\gamma^p$. In hypotheses [19-21] for describing anomalously rapid fading of elastic precursors, apart from multiplication there is introduction of heterogeneous generation of dislocations in a tangential stress field

at crystalline lattice defects. In [21], where both of these processes are summed, $N_m = N_{0m} + M\gamma^p + (\tau - \tau^*)/q$. The relative role of different factors affecting the increase in mobile dislocation density under wave deformation conditions is not yet clear since specific mechanisms for their formation have not been revealed. However, it is well known that about 10% of plastic deformation energy W^p is conserved in the form of elastic energy of point and linear defects. Therefore it is natural that dislocation density is represented only by function W^p, e.g., in the form

$$N_m = N_{0m} + \beta (W^p/a_0^2)^n. \tag{2.15}$$

Here a_0 is volumetric sound velocity under normal conditions; derivative $\dot{W}^p = 2S\dot{\gamma}^p/\rho$.

The structure of Eq. (2.15) reflects the tendency towards an increase in mobile dislocation density, and with $n < 1$ to retardation of this process as a result of dislocation blocking. Coefficient β and index n in (2.15) are free parameters of the FE determined from experimental data.

3. Steady-State SW Profiles. For media with linear D(u)-equations of the Hugoniot adiabat [22] [D(u) is SW velocity; u is mass velocity] relaxation relationships for the SW front and mathematical models of the front are particularly simple and convenient for interpreting the shape from an experiment using the analytical shape of deviators suggested in [23].

The structure of the front in relaxing media applied to gases with flow excitation of degrees of freedom was first considered in [24] and applied to solids in [25-30] devoted to the question of mathematical theory in [25-27] for SW in media with linear relaxation (t_p = const) [28], a generalized Maxwellian liquid with variable viscosity [29], and a dislocation model for a wave of small anharmonicity [30]. Two classes of solution were detected: with a continuous profile for weak SW with propagation rate D less than longitudinal sound velocity c_{L0}, and a solution with an internal break for a strong wave outstripping the elastic precursor. The sequence of the states of shock discontinuities form Rayleigh–Michaelson straight lines R in p–v-diagrams. For weak waves the wave rays commence a pole 1 (Fig. 1) on adiabat I at the elastic precursor amplitude, and they finish on plastic adiabat p^+ separated from equilibrium adiabat L by deviator $S^* = 4\tau^*/3$. For waves of the prescribed amplitude the hatched segment isolates the relaxing part of deviators $\pi = S - S^*$ included between wave straight line R and the shock adiabat.

If S^* = const and shock compressibility for a metal is described by a linear relationship $D(u) = a_0 + a_1 u$, according to [23]

$$\pi \approx 2\rho_1 a_1 (u - u_1)(u_2 - u_1), \tag{3.1}$$

where u is variable mass velocity at the wave front; u_2 is final velocity of Hugoniot condition 2; u_1 and ρ_1 are mass velocity and density of the elastic precursor. At a central point of the profile with $u = (u_1 + u_2)/2$, $d\pi/du = 0$ and maximum deviator

$$\pi_{1/2} \approx (1/2)\rho_1 a_1 (u_2 - u_1)^2. \tag{3.2}$$

Expressions (3.1) and (3.2) are approximate, but their difference from accurate relationships for the whole range of weak waves does not exceed several percent.

Differential equation of the profile $\frac{d\zeta}{du} = -\left(\frac{4}{3}\mu - D\frac{d\pi}{du}\right)\frac{t_p(\pi)}{\pi}$ represents fundamental Eq. (2.3) for a wave variable $\zeta = x - Dt$ (x is coordinate, t is time), obtained by the substitutions $S - S^* = \pi$, $\dot{S} = \dot{\pi} - D\frac{d\pi}{du}\frac{du}{d\zeta}$, $\dot{e} = -\frac{du}{d\zeta}$, and its equivalent shape will be

$$\frac{d\zeta}{du} = -\frac{1}{2\dot{\gamma}^p}\left(1 - \frac{3}{4}\frac{D}{\mu}\frac{d\pi}{du}\right). \tag{3.3}$$

A changeover to dimensionless velocity $\tilde{v} = (u - u_1)/(u_2 - u_1)$ and substitution of π from (3.1) leads to (3.3) to the form

$$\frac{1}{D}\frac{d\zeta}{d\tilde{u}} = -\frac{\alpha - 1 + 2\tilde{u}}{\tilde{u}(1 - \tilde{u})} t_p(\tilde{u}) \tag{3.4}$$

with a value

$$\alpha = \frac{2}{3}\frac{\mu}{a_1(p_2 - p_1)}. \tag{3.5}$$

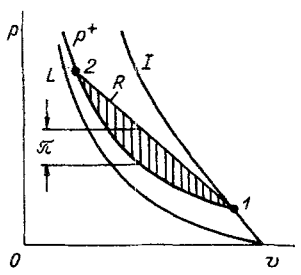

Fig. 1

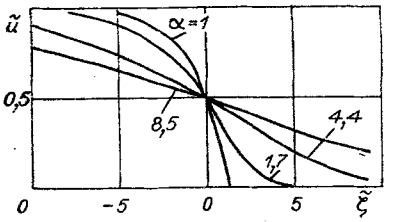

Fig. 2

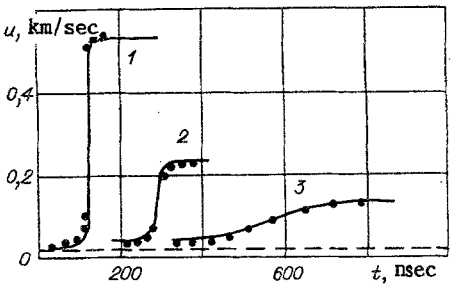

Fig. 3

For a wave of different amplitude parameters α with increasing D from a_0 to the initial longitudinal sound velocity c_{L0} change from ∞ to ~1.

Experimental recording of steady-state profiles determines the relaxation parameters for the averaged level of the front. With $\tilde{u} = 1/2$ the tangent at this point by intersecting with the horizontals $\tilde{u} = 0$ and 1 fixes in Euler coordinates the effective width of the front

$$\Delta_\zeta = (d\zeta/d\tilde{u})_{1/2} = 4\alpha D(t_p)_{1/2}. \tag{3.6}$$

Experimentally measured Δ_t for Lagrangian generators on the basis of (3.5) and (3.6) determines local relaxation time

$$(t_p)_{1/2} = \frac{3a_1}{8}\frac{\rho_1}{\rho_2}\frac{p_2 - p_1}{\mu_{1/2}}\Delta_t \tag{3.7}$$

and local viscosity

$$\eta_{1/2} = \frac{3a_1}{4}\frac{\rho_1}{\rho_2}(p_2 - p_1)\Delta_t. \tag{3.8}$$

Correspondingly the local plastic deformation velocity is

$$(\dot{\gamma}^p)_{1/2} = \frac{1}{2}\frac{u_2 - u_1}{D\Delta_t}\frac{\rho_2}{\rho_1}. \tag{3.9}$$

This last relationship makes it possible with a selected relationship $v(\tau)$ to find from (2.7) the density of mobile dislocations N_m.

The model of an ideal relaxing medium is realized with t_p = const and α = const. Under these assumptions after integrating (3.3) as in [30],

$$\tilde{\xi} = \ln\,[4(1 - \tilde{u})^{\alpha+1}\tilde{u}^{1-\alpha}],\ \tilde{\xi} = \zeta/(Dt_p). \tag{3.10}$$

For very weak wave with $\alpha \gg 1$

$$\tilde{u} = (1/2)[1 - \mathrm{th}\,(\tilde{\xi}/2\alpha)]. \tag{3.11}$$

Equation (3.11) describes the structure of a steady-state front in a viscous Newtonian liquid. In another limiting case at the upper boundary of the region of weak waves with α = 1

$$\tilde{u} = 1 - (1/2)\exp(\tilde{\xi}/2). \tag{3.12}$$

According to (3.12) in the wave movement direction the front has a finite size $\tilde{\zeta}(0) = 2\ln 2$. A typical configuration for steady-state profiles in an "ideal" medium for different α is shown in Fig. 2. Solutions (3.10)-(3.12) obtained in simplified ideas about the propagating medium are attractive in their simplicity and useful for qualitative interpretation of an experiment.

In another more realistic model of the medium suggested in [14] deformation velocity

$$\dot{\gamma}^p = A'\tau_v^2 \tag{3.13}$$

is connected with the active part tangential stresses τ_V by a quadratic relationship leading to a variable relaxation time $t_p = (2\mu A'\tau_V)^{-1}$.

At a central point of the profile

$$(t_p)_{1/2} = (4/3)[\mu A' a_1\rho_1(u_2 - u_1)^2]^{-1} \tag{3.14}$$

and in other conditions at the front

TABLE 1

Metal	γ_0	a_0, km/sec	a_1	c_{L0}, km/sec	v_s, km/sec	b, nm	B, Pa·sec	τ_0, GPa
Al	2,14	5,333	1,356	6,52	3,26	0,286	5,7	0,324
Be	1,16	7,993	1,132	13,13	9,03	0,228	2,0	0,396

TABLE 2

u_2-u_1, km/sec	p_2-p_1	$\pi_{1/2}$	$\mu_{1/2}$	Δ_t, nsec	$(t_p)_{1/2}$, nsec	$\eta_{1/2}$, Pa·sec	$(\dot{\gamma}^p)_{1/2}$, 1/sec	$N_m\cdot10^{-8}$, 1/cm²
	GPa							
				Al				
0,111	1,65	0,023	32	250	6,6	420	$4\cdot10^4$	19
0,213	3,25	0,087	34	31	1,5	100	$6\cdot10^5$	25
0,51	8,35	0,49	42	6	0,6	50	$6{,}6\cdot10^5$	40
				Be				
0,333	5,11	0,12	160	30	0,41	130	$1{,}6\cdot10^6$	3,8
0,61	9,84	0,89	174	22	0,53	185	$4{,}6\cdot10^6$	4,5
0,92	15,43	0,89	184	11	0,39	150	$7\cdot10^6$	5,5
1,37	24,27	1,98	200	4	0,18	70	$2\cdot10^7$	7

$$t_p(\tilde{u}) = (t_p)_{1/2}[4\tilde{u}(1-\tilde{u})]^{-1}. \tag{3.15}$$

Differential Eq. (3.4) after substituting t_p from (3.15) is transformed into a new equation

$$\frac{1}{D}\frac{d\zeta}{d\tilde{u}} = -\frac{\alpha-1+2\tilde{u}}{4\tilde{u}^2(1-\tilde{u})^2}(t_p)_{1/2}, \tag{3.16}$$

where $(t_p)_{1/2}$ is constant for all of the front conditions, but in contrast to an ideal relaxing medium it decreases according to (3.14) inversely proportional to the plastic wave amplitude. Equation (3.16) is integrated, as a result of which

$$4\frac{t}{(t_p)_{1/2}} = \frac{1}{\tilde{u}(1-\tilde{u})} - 4 + \alpha\left[\frac{2\tilde{u}-1}{\tilde{u}(1-\tilde{u})} - 2\ln\frac{1-\tilde{u}}{\tilde{u}}\right]. \tag{3.17}$$

4. Fundamental Equations for Aluminum and Beryllium. For aluminum experimental SW profiles [11], recorded at normal pressures of 9, 3.7, and 2.1 GPa, are reproduced in u–t-variables in Fig. 3 by curves 1-3, respectively. Similar front contours 1-4 for beryllium [12] in Fig. 4 relate approximately to SW amplitudes 6, 10, 17, and 25 GPa. The zero levels of reckoning plastic waves, coinciding with the plastic precursor amplitudes, are noted by broken lines. For aluminum

$$u_1 = 0.023\,\text{km/sec},\ p_1 = 0.41\,\text{GPa},\ S_1 = S^* = 0.133\,\text{GPa}; \tag{4.1}$$

and for beryllium

$$u_1 = 0.054\,\text{km/sec},\ p_1 = 1.31\ \text{GPa},\ S_1 = S^* = 0.83\,\text{GPa}. \tag{4.2}$$

Given in Table 1 are the rest of the characteristics for aluminum and beryllium in the original condition required for further analysis [Grüneisen coefficients γ_0, coefficients a_0, a_1, D(u)-relationships, and c_{Lo}, v_s, b, B, τ_0], and Table 2 are parameters for the steady-state shock waves being studied: amplitudes $u_2 - u_1$ for plastic waves measured from their graphs, calculated from pressures $p_2 - p_1 = \rho_1 D(u_2 - u_1)$, $D = a_0 + a_1(u_2 - u_1)$, maximum deviators $\pi_{1/2}$ from (3.2) and experimental time intervals Δ_t, characteristics relating to the central point of the profile, i.e., $\mu_{1/2}$ from data in [31, 32] for aluminum, and [33, 34] for beryllium, and calculated from values of Δ_t in Eqs. (3.7)-(3.9), $(t_p)_{1/2}$, $\eta_{1/2}$, and $(\dot{\gamma}^p)_{1/2}$.

As the results of analysis show, with an increase in amplitude and SW deviators velocity $\dot{\gamma}^p$ for aluminum increases by approximately two orders of magnitude, and for beryllium by a factor of thirty.

There is also a marked reduction in front dimension Δ_t. Viscosity decreases to several tens of pascal-seconds and relaxation time to fractions of a nanosecond. The dependences obtained $\tau_{1/2} - \dot{\gamma}^p_{1/2}$ are shown graphically in Fig. 5. For aluminum (curve 3) in accordance

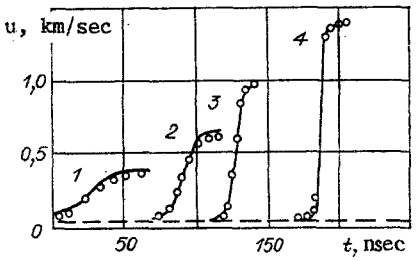

Fig. 4

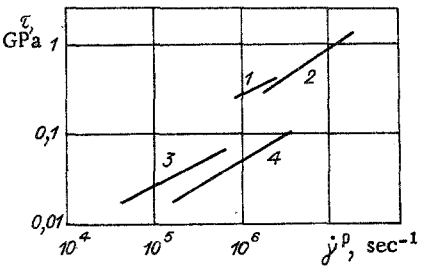

Fig. 5

with [14] the relaxation rate is approximately proportional to $\tau_{1/2}^2$, and for beryllium (curve 2) to $\sim\tau^{3/2}$. Lines 1 and 4 are results from [14] for iron and copper, given here under our treatment.

Dislocation models and FE are found from data in Table 2 and experimental plastic wave profiles. For aluminum the optimum description of the whole experiment is achieved with substitution in (2.7) of Eq. (2.13) for dislocation velocity and for dislocation density, respectively,

$$N_m(\mathrm{Al})\cdot 10^{-8}\,\mathrm{cm}^{-2} = 10^{-2} + 410\,(W^p/a_0^2)^{0,3}. \tag{4.3}$$

For beryllium optimum equations are (2.11) and

$$N_m(\mathrm{Be})\cdot 10^{-8}\,\mathrm{cm}^{-2} = 10^{-2} + 43.5\,(W^p/a_0^2)^{0,3}. \tag{4.4}$$

"Dislocation" profiles (shown by points, correspondingly, in Figs. 3 and 4) calculated by Eqs. (2.13), (4.3), (2.11), (4.4) using parameters in Table 2 agree satisfactorily with experimental curves. Nanosecond relaxation times and low viscosity are caused by the considerable mobile dislocation density formed during shock compression. For a metal behind the SW front values of N_m are calculated by Eqs. (4.3) and (4.4).

For aluminum everywhere $N_m > 2\cdot 10^9$ cm^{-2}. For beryllium N_m is greater than $4\cdot 10^8$ cm^{-2}. On the basis of the FE obtained plastic deformation rate behind the SW front is connected with viscous stresses by the relationships

$$\dot\gamma^p(\mathrm{Al}) = N_m b^2 v_s z^2 (1+z^2)^{-1}; \tag{4.5}$$

$$\dot\gamma^p(\mathrm{Be}) = N_m b^2 v_s [(1+z^2)^{1/2} - 1] z^{-1}. \tag{4.6}$$

Numerically with N_m (see Table 2) and $z \le 0.5$

$$\dot\gamma^p(\mathrm{Al}) = \frac{4N_m b^2}{v_s}\left(\frac{\tau_v}{B}\right)^2 \geqslant 1{,}8\cdot 10^8 \tau_v; \tag{4.7}$$

$$\dot\gamma^p(\mathrm{Be}) = \frac{N_m b^2}{B}\tau_v \geqslant 10^7 \tau_v. \tag{4.8}$$

In unloading waves and repeated compression with deformation velocity $\sim 10^6$ sec^{-1} viscous components of tangential stresses in beryllium and aluminum estimated by (4.7) and (4.8) do not exceed 0.1 GPa.

Rheological parameters for SW of equal amplitude relate to different structural states of the metal. Combination of them [14] in universal relationships of the form $\dot\gamma^p = A'\tau_v^2$ do not have a strict basis, nonetheless experimental data placed in Eq. (3.13) relating to average shock pressure levels, according to the determination provide a correct description of front curvature and the known extent of profile configuration. As an illustration shown in Fig. 6 are dimensionless $\tilde u(t)$-profiles for an SW in aluminum for 2.1 GPa and in Fig. 7 in beryllium for 0.6 GPa. Curves were calculated by Eq. (3.17) and values of $(t_p)_{1/2}$ in Table 2; points are experimental data [11, 12]. The model of (3.13) suggested in [14] markedly reduces relaxation rate.

5. Discussion. The equations obtained determine the resistance of aluminum and beryllium to shear over wide ranges of deformation rate and for different levels of defects in their structure, i.e., with the existence of different dislocation densities. For the dislocation structure formed in the metal by compressive shock pressures of several gigapascal or more, the high dislocation density markedly decreases metal viscosity and the value of the ductile components of tangential stresses to small fractions of a gigapascal with shear deformation rates $\sim 10^6$ sec^{-1}.

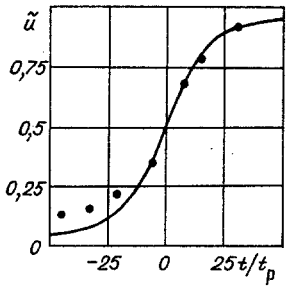

Fig. 6

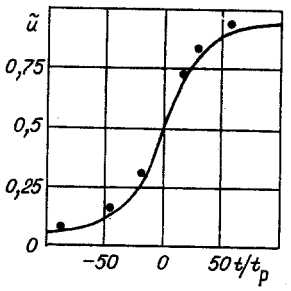

Fig. 7

This conclusion is based on the behavior of metals under the action of high SW front tangential stresses. Due to the change in number of mobile dislocations, the applicability of the FE constructed to subsequent deformation processes in loading waves and repeated loading is not apparent [13]. The role of viscosity and relaxation for a metal saturated with shock-compressive dislocations is explained independently with the exception of wave pulses of different time scale created with geometric similarity for a different deformation rate. This class of experiments relates to the well-known studies for the corrugated front method [35, 36] where viscosities ~10^4 Pa·sec were found from the disturbance of similarity in a decaying perturbation of different wavelength. These last studies [37] for viscosity of water have shown however that in the process of perturbation decay shock reactions play a more complex role than simple viscous dissipation.

In more direct tests the effect of loading rate on the resistance of aluminum appeared to be insignificant at shock pressures of 2 GPa [38] and it did not develop at 15 GPa [39]. Tests [13] were interpreted in [40] for SW reflection from a free surface. Attention was drawn to the difference in unloading velocity of different metal layers, decreasing with their distance from the free surface. As calculations have shown, the initial minimum movement velocity for the surface increases as signals arrive from deeper layers. The period of nonsteady movement for a barrier is approximately equal to the relaxation time, and from experimental data [13] it does not exceed several nanoseconds. In aggregate experiments confirm the estimates made above for viscous resistance at high deformation rates.

In the present study critical deviators S* for the wave front are taken to be constant and equal to the elastic precursor deviators $S^* = S_1 = \frac{2}{3}\frac{1-2\sigma}{1-\sigma}p_1$ (σ is Poisson's ratio). The most direct method for determining the stress tensor behind the wave front and checking the assumptions made involves simultaneous measurement of two principal stresses, i.e., normal and parallel to the wave front. The first record of this type was accomplished in [41] in steel specimens in two perpendicular electrostatic sensors. In the range 9 GPa a constant value Y = 0.56 GPa was recorded. Similar results (0.5 GPa) were given by similar measurements in [42] by managing sensors in contrast to [43] where by the same procedure higher Y were related to unrealistic volumetric compression curves.

For aluminum and beryllium deviators behind the SW front have been determined by the p–v-trajectory method [44] and an equivalent "self-conforming method" [45]. Small deviators close to S_1 have been recorded for aluminum up to shock pressures of 22 GPa and for beryllium [46] up to 35 GPa.

The most probable reason for forming these quasistatic conditions behind the front is short-term metal loss of strength due to local release of heat along slip planes. According to estimates in [47] the time for temperature leveling and strength recovery for aluminum is ~10^{-8} sec. Formally this process is described [40] by "cooling" of generated "hot" dislocations N_h whose number varies with velocity $\dot{N}_h = N_m - N_h/T_p$. In the characteristic time for thermal relaxation T_p the critical stress τ^* evolves from an initial value τ_1^* to an equilibrium value τ_2^* according to a relationship of the form

$$\tau^* = \tau_1^* + 2(\tau_2^* - \tau_1^*)\left[1 + \exp\frac{N_h}{N_m - N_h}\right]^{-1}.$$

For aluminum the equilibrium yield strength $Y_2 = 2\tau_2^*$ in the function due to pressure from the data of different researchers is given in [41]. An increase in Y_2 commences with a shock pressure of 8 GPa and with an SW amplitude of 23 GPa it reaches 1.3 GPa. For beryllium [46] with 35 GPa, Y = 2.5 GPa.

As comparison of these values with the magnitude of viscous components shows, as the number of mobile dislocations increases the model for a metal relaxing according to its own character in quasistatics and with low SW amplitudes "degenerates" into a model of a strengthening elastoplastic medium whose principal characteristic is an effective yield limit.

LITERATURE CITED

1. V. M. Fokin and E. M. Khakimov, "Numerical modeling of compressive and rarefaction waves in metals," Zh. Prikl. Mekh. Tekh. Fiz., No. 5 (1979).
2. L. A. Merzhievskii and A. D. Resnyanskii, "Selection of a model for describing attenuation of shock waves in metals," Fiz. Goreniya Vzryva, No. 1 (1983).
3. D. J. Steinberg, S. G. Cochran, and H. W. Guinan, "A constitutive model for metals applicable at high strain rate," J. Appl. Phys., 51, No. 3 (1980).
4. S. K. Godunov, Elements of Solid Mechanics [in Russian], Nauka, Moscow (1978).
5. G. I. Kanel', "Model of plastic deformation kinetics for metals under shock-wave loading conditions," Zh. Prikl. Mekh. Tekh. Fiz., No. 2 (1982).
6. I. V. Simonov and B. S. Chekin, "High-velocity impact of iron plates," Fiz. Goreniya Vzryva, No. 2 (1975).
7. L. V. Al'tshuler and B. S. Chekin, "Relaxation parameters for metals behind the front of shock waves," in: Detonation [in Russian], Chernogolovka (1978).
8. D. R. Carran, "Nonhydrodynamic attenuation of shock waves in aluminum," J. Appl. Phys., 34, No. 9 (1963).
9. J. O. Ercman and A. B. Christensen, "Attenuation of shock waves in aluminum," J. Appl. Phys., 38, No. 13 (1967).
10. L. V. Al'tshuler, M. I. Brazhnik, and G. S. Telegin, "Strength and elasticity of iron and copper with high compressive shock pressures," Zh. Prikl. Mekh. Tekh. Fiz., No. 6 (1971).
11. J. N. Johnson and L. M. Barker, "Dislocation dynamics and steady plastic wave profiles in 6061-T6 aluminum," J. Appl. Phys., 40, No. 11 (1969).
12. J. R. Asay, L. C. Chhabildas, and J. L. Wise, "Strain effects in beryllium under shock compression," in: Shock Waves in Condensed Matter, H. C. Wolfe (ed.), Amer. Inst. Phys., N.Y. (1982).
13. L. C. Chhabildas and J. R. Asay, "Rise-time measurements of shock transition in aluminum, copper, and steel," J. Appl. Phys., 50, No. 4 (1979).
14. J. W. Swegle and D. E. Grady, "Shock viscosity in the prediction of shock wave rise times," J. Appl. Phys., 52, No. 2 (1985).
15. L. E. Malvern, "Plastic wave propagation in a bar of material exhibiting a strain rate effect," Q. Appl. Math., 8, No. 4 (1951).
16. H. E. Read, "A microdynamical approach to constitutive modeling of shock induced deformation," in: Metallurgical Effects at High Strain Rates, Plenum Press (1973).
17. P. P. Gillis, J. J. Gilman, and J. W. Taylor, "Stress dependences of dislocation velocities," Philos. Mag., 20, 279 (1969).
18. J. W. Taylor, "Dislocation dynamics and dynamic yielding," J. Appl. Phys., 36, No. 10 (1965).
19. Y. M. Gupta, "Dislocation mechanisms for stress relaxation in shocked LiF," J. Appl. Phys., 46, No. 2 (1975).
20. J. R. Asay, D. L. Hicks, and D. B. Holdridge, "Comparison of calculated and experimental elastic-plastic wave profiles in LiF," J. Appl. Phys., 46, No. 10 (1975).
21. P. V. Makarov, T. M. Platova, and V. A. Skripnyak, "Plastic deformation and microstructural transformations of metals in shock waves," Fiz. Goreniya Vzryva, No. 5 (1983).
22. L. V. Al'tshuler, A. A. Bakanova, et al., "Shock adiabats for metals. New data, statistical analysis, and general regularities," Zh. Prikl. Mekh. Tekh. Fiz., No. 2 (1981).
23. E. A. Dynin, "Questions of shock pulse propagation in condensed media," Diss. Cand. Phys.-Mat. Sci., VNIIOFI, Moscow (1978).
24. Ya. B. Zel'dovich, Theory of Shock Waves and Introduction to Gas Dynamics [in Russian], Izd. AN SSSR, Moscow (1946).
25. S. K. Godunov and N. S. Kozin, "Structure of shock waves in a viscoelastic medium with nonlinear dependence of Maxwellian viscosity on substance parameters," Zh. Prikl. Mekh. Tekh. Fiz., No. 5 (1974).
26. A. I. Gulidov, V. M. Fomin, and N. N. Yanenko, "Structure of compressive waves in inelastic media," Izv. Akad. Nauk SSSR, Mekh. Tverd. Tela, No. 5 (1975).
27. V. G. Grigor'ev, A. S. Nemirov, and V. K. Sirotkin, "Structure of shock waves in elastoplastic relaxing media," Zh. Prikl. Mekh. Tekh. Fiz., No. 1 (1979).

28. J. M. Kelly and P. P. Gillis, "An ideally viscoplastic analysis of shock profiles," Acta Mech., 26, 47 (1977).
29. N. S. Kozin and N. K. Kuz'mina, Shock Adiabats and the Structure of Shock Waves in Iron [in Russian], VTs SO AN SSSR, Novosibirsk (1975).
30. E. A. Dynin, "Analytical study of steady-state compressive wave profiles in media with a dislocation plastic relaxation mechanism," Izv. Akad. Nauk SSSR, Mekh. Tverd. Tela, No. 2 (1981).
31. D. Yaziv, Z. Rosenberg, and Y. Parton, "A variation of the elastic constants of 2024-T351 Al under dynamic pressures," J. Appl. Phys., 53, No. 1 (1982).
32. T. E. Arvidson, Y. M. Gupta, and G. E. Duval, "Precursor decay in 1060 aluminum," J. Appl. Phys., 46, No. 10 (1975).
33. J. L. Wise, L. S. Chhabildas, and J. R. Asay, "Shock compression of beryllium," in: Shock Waves in Condensed Matter, H. C. Wolfe (ed.), Amer. Inst. Phys., N.Y. (1982).
34. L. C. Chhalbidas, J. L. Wise, and J. R. Asay, "Reshock and release behavior of beryllium," in: Shock Waves in Condensed Matter, H. C. Wolfe (ed.), Amer. Inst. Phys., N.Y. (1982).
35. A. D. Sakharov, R. M. Zaidel', V. N. Mineev, and A. G. Oleinik, "Experimental study of the stability of shock waves and mechanical properties of a substance at high pressures and temperatures," Dokl. Akad. Nauk SSSR, 159, No. 5 (1964).
36. V. N. Mineev and R. M. Zaidel', "Viscosity of water and mercury under shock loading," Zh. Éksp. Tekh. Fiz., 54, No. 6 (1968).
37. G. Kh. Kim, "Measurement of the viscosity of shock-compressed water," Zh. Prikl. Mekh. Tekh. Fiz., No. 5 (1984).
38. J. Lipkin and J. R. Asay, "Reshock and release of shock-compressed 6061—T6 aluminum," J. Appl. Phys., 47, No. 1 (1977).
39. G. I. Kanel', A. N. Dremin, and O. B. Chernikova, "Resistance to plastic deformation of aluminum AD-1 and duralumin D16 under shock compression conditions," Zh. Prikl. Mekh. Tekh. Fiz., No. 4 (1981).
40. L. V. Al'tshuler and B. S. Chekin, "Rheology of the wave deformation of materials," Fiz. Goreniya Vzryva, No. 5 (1983).
41. G. V. Stepanov and V. V. Astanin, "Determination of the resistance of a material to shear behind a plane shock-wave front," Probl. Prochn., No. 4 (1976).
42. P. F. Chartagnac, "Determination of mean and deviatoric stresses in shock loaded solids," J. Appl. Phys., 53, No. 2 (1982).
43. S. A. Novikov, "Shear stress and spalling strength of materials under shock loads," Zh. Prikl. Mekh. Tekh. Fiz., No. 3 (1981).
44. A. N. Dremin and G. I. Kanel', "Rarefaction waves in shock-compressed metals," Zh. Prikl. Mekh. Tekh. Fiz., No. 2 (1976).
45. J. R. Asay and L. C. Chhabildas, "Determination of the shear strength of shock compressed 6061—T6 aluminum," in: Shock Waves and High Strain Rate Phenomena in Metals, A. Mayers and L. E. Murr (eds.), Plenum Press (1981).
46. W. C. Moss, "The effect of material strength on determining pressures 'on' and 'off' the Hugoniot," J. Appl. Phys., 55, No. 1 (1984).
47. D. E. Grady and J. R. Asay, "Calculation of thermal trapping in shock deformation on aluminum," J. Appl. Phys., 53, No. 11 (1982).